POLITECNICO DI TORINO
Repository ISTITUZIONALE

Assessment of multi-phase IPM for low-voltage battery electric powertrain

Original
Assessment of multi-phase IPM for low-voltage battery electric powertrain / Aguilar-Zamorate, I.S., Manca, R., Favelli, S., Tramacere, E., Galluzzi, R., Tonoli, A.. - (2024), pp. 1-6. (2024 International Symposium on Electromobility (ISEM) Guadalajara (MEX) 18-20 September 2024) [10.1109/isem62699.2024.10786598].

Availability:
This version is available at: 11583/2995246 since: 2024-12-12T13:23:31Z

Publisher:
IEEE

Published
DOI:10.1109/isem62699.2024.10786598

Terms of use:

This article is made available under terms and conditions as specified in the corresponding bibliographic description in the repository

Publisher copyright
IEEE postprint/Author's Accepted Manuscript

©2024 IEEE. Personal use of this material is permitted. Permission from IEEE must be obtained for all other uses, in any current or future media, including reprinting/republishing this material for advertising or promotional purposes, creating new collecting works, for resale or lists, or reuse of any copyrighted component of this work in other works.

(Article begins on next page)

18 November 2026

Assessment of multi-phase IPM for low-voltage battery electric powertrain

Irving S. Aguilar-Zamorate
School of Engineering and Sciences
Tecnologico de Monterrey
Mexico City, Mexico
a01336855@tec.mx

Raffaele Manca
Center for Automotive Research and Sustainable Mobility (CARS)
Politecnico di Torino
Turin, Italy
raffaele.manca@polito.it

Stefano Favelli
Center for Automotive Research and Sustainable Mobility (CARS)
Politecnico di Torino
Turin, Italy
stefano.favelli@polito.it

Eugenio Tramacere
Center for Automotive Research and Sustainable Mobility (CARS)
Politecnico di Torino
Turin, Italy
eugenio.tramacere@polito.it

Renato Galluzzi
School of Engineering and Sciences
Tecnologico de Monterrey
Mexico City, Mexico
renato.galluzzi@tec.mx

Andrea Tonoli
Center for Automotive Research and Sustainable Mobility (CARS)
Politecnico di Torino
Turin, Italy
andrea.tonoli@polito.it

***Abstract*—The ongoing evolution in electric vehicle (EV) technology underscores the critical role of advancing motor architectures to enhance efficiency and reliability. Multiphase motors are emerging as pivotal solutions in low-voltage systems, offering enhanced efficiency, reliability, and adaptability compared to traditional three-phase configurations.**

This study assesses the performance of a multiphase Interior Permanent Magnet (IPM) motor for traction applications in a low-voltage battery EV operating at 48V. The research contrasts the performance of a six-phase IPM motor against a conventional three-phase IPM motor. Key metrics such as torque characteristics, energy consumption, and efficiency across various driving cycles are compared and analyzed.

Results indicate that the six-phase configuration offers improved torque characteristics with reduced ripple, enhancing vehicle dynamics and efficiency. The study also highlights the benefits of multiphase motors in terms of fault tolerance and torque density, which are crucial for optimizing performance in 48V systems. Comparative analysis demonstrates the suitability of multiphase motors for future EV traction applications, despite current limitations in comprehensive studies and practical implementations.

***Index Terms*—Multiphase traction motors, Interior Permanent Magnet, Low voltage, Battery electric vehicle, Driving cycle.**

I. Introduction

The ongoing evolution in electric vehicle (EV) technology emphasizes the critical advancement of motor and powertrain architectures to enhance efficiency and reliability [1]. Among these advancements, multiphase motors are emerging as pivotal solutions, particularly in low-voltage systems, offering significant advantages in efficiency, reliability, and adaptability.

In urban scenarios, low-voltage L-class vehicles are increasingly favored in micro-mobility and shared mobility applications due to their compact size and cost-effectiveness [2]. However, concerns regarding safety standards and adaptability to extra-urban missions persist [3]. Addressing these challenges underscores the need for a sustainable and affordable vehicle tailored for urban operations yet capable of reconfiguration for extra-urban missions. Such a vehicle should merge the low-voltage characteristics typical of L-category vehicles with the safety, range, and performance features associated with M-category vehicles, bridging the gap between these vehicle classes [4]. Indeed, this categorization is aligned with the European Union where the L-category corresponds to 2- or 3-wheel vehicles and quadricycles whereas the M-category is for vehicles carrying passengers [5]. Additionally, a DC link battery voltage below 60 V facilitates manual battery swap functionalities in a safe environment.

Achieving this balance between low-voltage operation and high-power traction capabilities necessitates innovative powertrain technology.

Central to enabling this versatility are multiphase motors and dual inverter solutions. Unlike traditional three-phase motors, multiphase motors offer enhanced fault tolerance, reduced power per phase, and improved torque density [6], which are crucial for optimizing performance in 48V systems [7]. Moreover, multiphase drives exhibit improved magnetomotive force distribution, thereby reducing torque ripple. Consequently, there is growing interest in both academic research [8] and industry applications [9] for employing multiphase motors in electric vehicle traction systems.

While state-of-the-art electric vehicles typically operate with high-voltage (HV) power systems with nominal voltages up to 600 V, low-voltage (LV) systems are predominantly utilized in hybrid electric vehicles or micro-mobility applications [10], as LV systems would require prohibitively high currents to fulfill complete driving cycles. In this context, multiphase drives emerge as a valuable solution for low-voltage and high-power

electric vehicles.

Thus, while initial explorations in the literature have addressed multiphase-drive systems in low-voltage applications [11], [12], comprehensive studies and practical implementations of low-voltage traction systems in battery electric vehicles remain limited. This paper aims to provide a comparative analysis between three-phase and six-phase drives for a low-voltage electric vehicle application, assessing the primary features and advantages of multiphase drives.

The paper is structured as follows: Section 2 details the specifications of the proposed electric drive and outlines the methodology used to develop the efficiency map. Section 3 presents numerical results comparing the performance of three-phase and six-phase configurations. Finally, conclusions are summarized in the last section.

II. Method

The methodology for the analysis is described according to the reference vehicle and electric drive specifications.

A. Vehicle specifications

The proposed vehicle concept aims to be safe, affordable, and tailored to user needs, featuring a reconfigurable low-voltage powertrain architecture. This reconfigurability is achieved through a battery swap system. The low-voltage design allows for safe manual swap operations and seamless integration of the battery modules with the domestic grid.

The main specifications of the case study vehicle are detailed in Table I. The vehicle features two 48-V swappable battery modules connected to a dual three-phase inverter, which powers a six-phase electric motor. The electric drive module includes a single-speed reducer. Each inverter is powered by a galvanically isolated DC link, which enables complete reconfigurability and ensures fail-safe operation.

To meet the typical performance standards of an M-class car while maintaining a voltage below 60 V, the adoption of a multi-phase drive is essential. The scheme of the proposed electric drive module is reported in Figure 1.

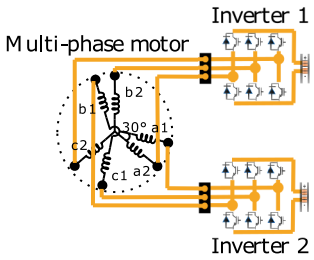


Fig. 1. Electric drive module scheme

B. Drive specifications

The selected drive is an interior permanent magnet synchronous motor (IPMSM) featuring an interior V-shape NdFeb N42H magnets, analyzed in Ansys Motor-CAD. The main drive specifications are outlined in Table II, while the cross-section geometry is presented in Fig. 2. The motor mass is equal for both configurations and refers to the active electromagnetic sections referring to the stator, winding armature, rotor, and magnets.

TABLE I
Vehicle specifications

Specification	Symbol	Value	Unit
Curb mass	m_{veh}	≥ 1000	kg
Static rolling coefficient	f_{r0}	5.3	N/kN
Drag coefficient	C_{d}	0.33	–
Gear ratio	τ_{gb}	10.2	–
Top speed	v_{max}	130	km/h
WLTC range	–	≥ 200	km
Nominal battery voltage	V_{dc}	48	V

TABLE II
Motor drive specifications

Specification	Symbol	Value	Unit
Stator slots	N_{s}	48	–
Pole pairs	p	4	–
DC link voltage	V_{dc}	48	V
Peak RMS phase current	–	450	A
Maximum speed	ω_{max}	14,000	r/min
Stator outside radius	R_{so}	85.5	mm
Stator inside radius	R_{si}	55.9	mm
Rotor inside radius	R_{ri}	33.7	mm
Air gap	g	0.7	mm
Motor mass (active)	W_{a}	14.6	kg

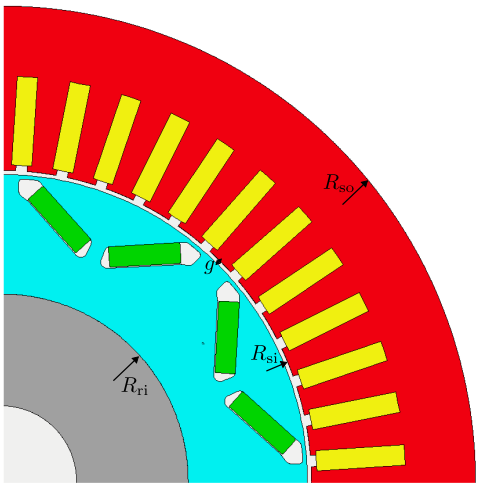


Fig. 2. Cross-section of the IPM used

The hairpin winding pattern for both systems is presented in Fig. 3 with both having a full pitch winding pattern. In particular, the six-phase machine has an asymmetrical winding configuration because the space angle between the two three-phase windings is 30°. The two neutral points are isolated thus zero-sequence currents cannot flow which improves the DC-link utilization and eases the current control [13]. Moreover, the multiphase configuration allows operation at different

faulty conditions [6] which highlights its superior robustness against a traditional three-phase configuration. Although the alternative single-neutral connection has larger torque ranges in fault operation than the two-neutral connection [13], the latter was chosen to achieve vehicle reconfiguration and fail-safe operations with dual inverter system.

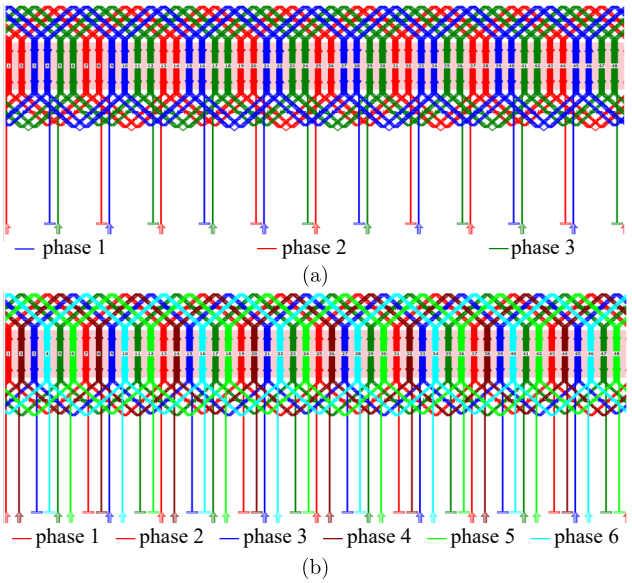


Fig. 3. Winding pattern for (a) three-phase and (b) six-phase

C. Efficiency map calculation

The maximum torque per ampere (MTPA) and maximum torque per volt (MTPV) strategies are used to derive the electromagnetic torque maps as a function of the drive speed (ω) [14]. For this purpose, the synchronous rotating frame (dq axes) in steady-state is employed [15]:

$$\begin{aligned} v_{\mathrm{d}} &= Ri_{\mathrm{d}} - p\omega_{\mathrm{m}}\lambda_{\mathrm{q}}(i_{\mathrm{d}}, i_{\mathrm{q}}) \\ v_{\mathrm{q}} &= Ri_{\mathrm{q}} + p\omega_{\mathrm{m}}\lambda_{\mathrm{d}}(i_{\mathrm{d}}, i_{\mathrm{q}}) \\ T_m &= \frac{3}{2}p\left(\lambda_{\mathrm{d}}(i_{\mathrm{d}}, i_{\mathrm{q}})\, i_{\mathrm{q}} - \lambda_{\mathrm{q}}(i_{\mathrm{d}}, i_{\mathrm{q}})\, i_{\mathrm{d}}\right) \end{aligned} \tag{1}$$

where d and q subscripts denote the machine axis for voltages (v), currents (i) and flux linkages (λ). In particular, the flux linkages maps are obtained through finite element analysis and they are a function of both dq axis currents to account for saturation effects.

Losses components for windings (DC and AC), iron, and magnets are accounted for in the calculation of the efficiency map. The DC winding losses are computed from the Joule loss equation using

$$P_{\mathrm{dc}} = 3R_{\mathrm{ph}}I_{\mathrm{ph}}^2\,[\mathrm{W}] \tag{2}$$

where $R_{\mathrm{ph}} = 1.47\Omega$ is the phase resistance and I_{ph} is the rms phase current. Alternatively, the AC winding losses are computed in Ansys Motor-CAD [16] considering proximity and skin effects, and the frequency dependence on them [16].

Bertotti iron-loss model method [17] is used to compute stator and rotor specific losses according to

$$P^*_{\mathrm{iron}} = k_{\mathrm{h}} f B^{3.701} + k_{\mathrm{eddy}} f^2 B^2 + k_{\mathrm{exc}} f^{1.5} B^{1.5}\,[\mathrm{W/kg}] \tag{3}$$

where the coefficients for hysteresis, eddy currents, and excess losses are $k_{\mathrm{h}} = 4.68 \cdot 10^{-3}$, $k_{\mathrm{eddy}} = 2.262 \cdot 10^{-6}$, and $k_{\mathrm{exc}} = 1.98 \cdot 10^{-3}$, respectively, for the M250-35A steel.

Volumetric magnet losses is calculated from the induced eddy current density J_{e} which is proportional to the change in the magnetic vector potential $\mathbf{A}$ with time t [16]:

$$P^*_{\mathrm{pm}} = \sigma_{\mathrm{pm}} \left(\frac{\partial \mathbf{A}}{\partial t}\right)^2\,[\mathrm{W/m^3}] \tag{4}$$

where $\sigma_{\mathrm{pm}} = 5.556 \cdot 10^5\,\mathrm{S/m}$ is the magnet conductivity. (4) is constrained to satisfy that the net total current flowing in each magnet be zero at any time instant [18].

Finally, the efficiency in the motor operating mode is calculated as the ratio of the mechanical power divided by the total input power

$$\eta_{\mathrm{m}} = \frac{T_{\mathrm{m}}\omega_{\mathrm{m}}}{T_{\mathrm{m}}\omega_{\mathrm{m}} + P_{\mathrm{w}} + P_{\mathrm{iron}} + P_{\mathrm{pm}}}. \tag{5}$$

III. Results

A. Steady state performance comparison

The first 15th electrical harmonics in the MMF are shown in Fig. 4. It is devised that the amplitude of the first harmonic is halved in the six-phase compared with the three-phase, while significantly lower in subsequent harmonics orders, except for the 5th and 7th harmonics. Since the MMF is mainly induced by the fundamental stator phase current, an increased phase number produces higher harmonic orders of the MMF with lower amplitudes [19].

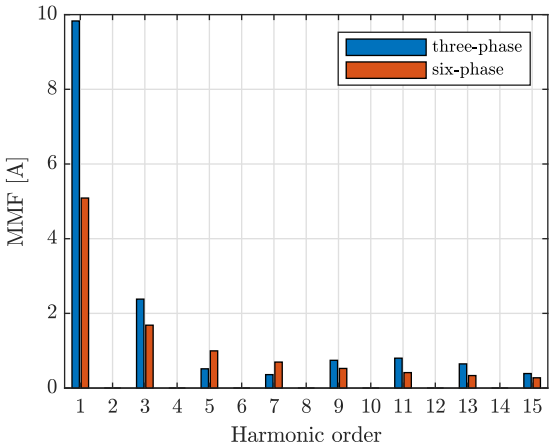


Fig. 4. Electrical harmonics

The electromagnetic torque density is shown in Fig. 5 corresponding to a shaft speed of $1,000\,\mathrm{r/min}$, an RMS phase current of $450\,\mathrm{A}$ and phase advance (current load angle) of $30\,\mathrm{deg}$. The RMS torque density is $4.88\,\mathrm{Nm/kg}$ with a ripple of $0.21\,\mathrm{Nm/kg}$ for the three-phase, while it has a

magnitude of $5.13\,\mathrm{Nm}$ and ripple of $0.12\,\mathrm{Nm}$ for the six-phase. Although the benefit in torque increase is marginal by having a six-phase configuration, about 5%, the torque ripple is halved representing a considerable improvement for vehicle dynamics. Indeed, the torque ripple is proportional to the harmonics content of the MMF [20], therefore it is attenuated in the six-phase system which agrees with the results obtained previously in Fig. 4.

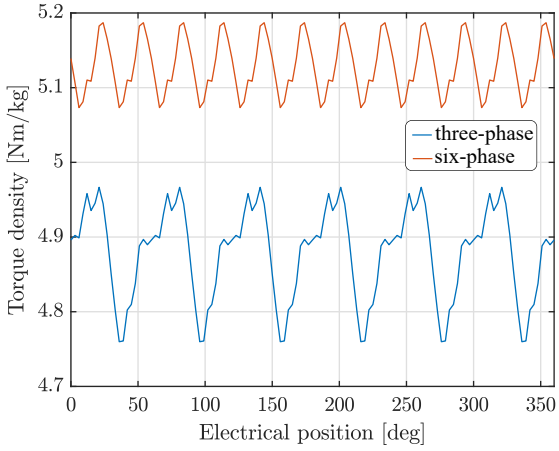


Fig. 5. Electromagnetic torque density

The back electromotive force (EMF) is presented in Fig. 6 for the working point studied in the electromagnetic torque. Since the number of turns in series per phase in the six-phase is half of the three-phase, the induced back EMF, which is proportional to the variation of the flux linkage, will follow this ratio.

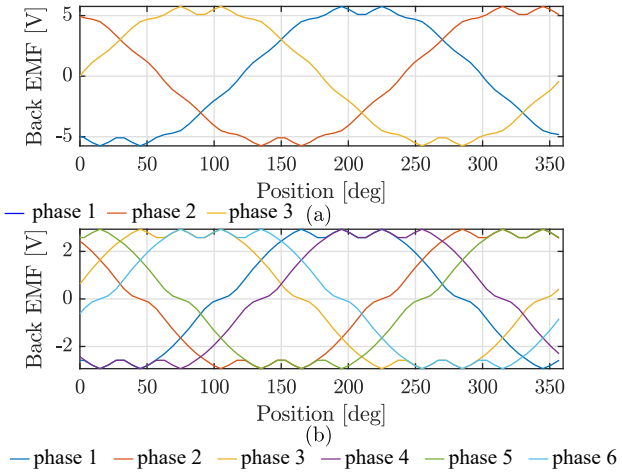


Fig. 6. Induced back EMF for the (a) three-phase and (b) six-phase machine.

B. Driving cycle performance comparison

Results for the achieved vehicle dynamics under the two configurations are presented in Table III. Regarding energy consumption, the six-phase is more efficient under the WLTC-city and WLTC driving cycles. The latter is aligned with the efficiency maps in Fig. 7 which shows that the last contour line corresponding to a top efficiency of 97% has a wider area in the six-phase than in the three-phase. Moreover, all the working points of the driving cycle are contained in the six-phase drive efficiency envelope, while in the three-phase some are outside. Consequently, the vehicle equipped with the three-phase drive would not be able to accomplish the WLTC driving cycle.

TABLE III
VEHICLE RESULTS FOR THREE- AND SIX-PHASE CONFIGURATIONS

Specification	Three-phase	Six-phase	Unit
Top speed	100	130	km/h
Energy WLTC-City	8.41	8.37	kWh/100km
Energy WLTC	12.77	12.67	kWh/100km
Torque at wheels	732	770	Nm
Acc. time: 0-100 km/h	26	16	s

Additionally, from Fig. 7, the base speed (boundary condition for field-weakening) is doubled in the six-phase arrangement compared with the three-phase which is around $3\,\mathrm{kr/min}$. A direct consequence is that the acceleration time from 0 to $100\,\mathrm{km/h}$ is drastically reduced in $10\,\mathrm{s}$ or 39% in the multiphase system respect the three-phase which is a substantial improvement from the driving perception. Furthermore, the top speed is increased by one-third, significantly improving the vehicle capabilities at high-way operation.

The peak power is doubled in the six-phase compared with the three-phase system, from Fig. 7. Aditionally, while the peak is around $8\,\mathrm{kr/min}$ for the three-phase and then starts to decrease, the peak in the six-phase is reached close to the maximum speed requirement of the drive around $13\,\mathrm{kr/min}$. Lastly, the maximum torque transferred to the wheels has a perceptible gain of 5% in the multiphase system.

IV. CONCLUSION

The contribution of this work resides in assessing the applicability of multiphase traction drives for low-voltage traction systems in battery electric vehicles at 48 V. Therefore, a comparative assessment between a three-phase and a six-phase IPM drive for previous target application has been performed which concludes that the multiphase arrangement has superior capabilities in terms of efficiency, reliability (fault-tolerance), adaptability (configurable for dual vehicle missions) and torque density.

The steady-state analysis highlights a lower content of electrical harmonics in the MMF for the multiphase solution. Consequently, the torque ripple has been halved in the six-phase while it has a superior magnitude compared with the three-phase. Moreover, the driving cycle evaluation outlines that the multiphase solution has better performance in the key metrics for energy consumption, top speed, torque transferred to the wheels, and acceleration time $(0-100\ \mathrm{km/h})$. Indeed, acceleration time has almost halved significantly gaining from the driving perception. The latter is the consequence of split-

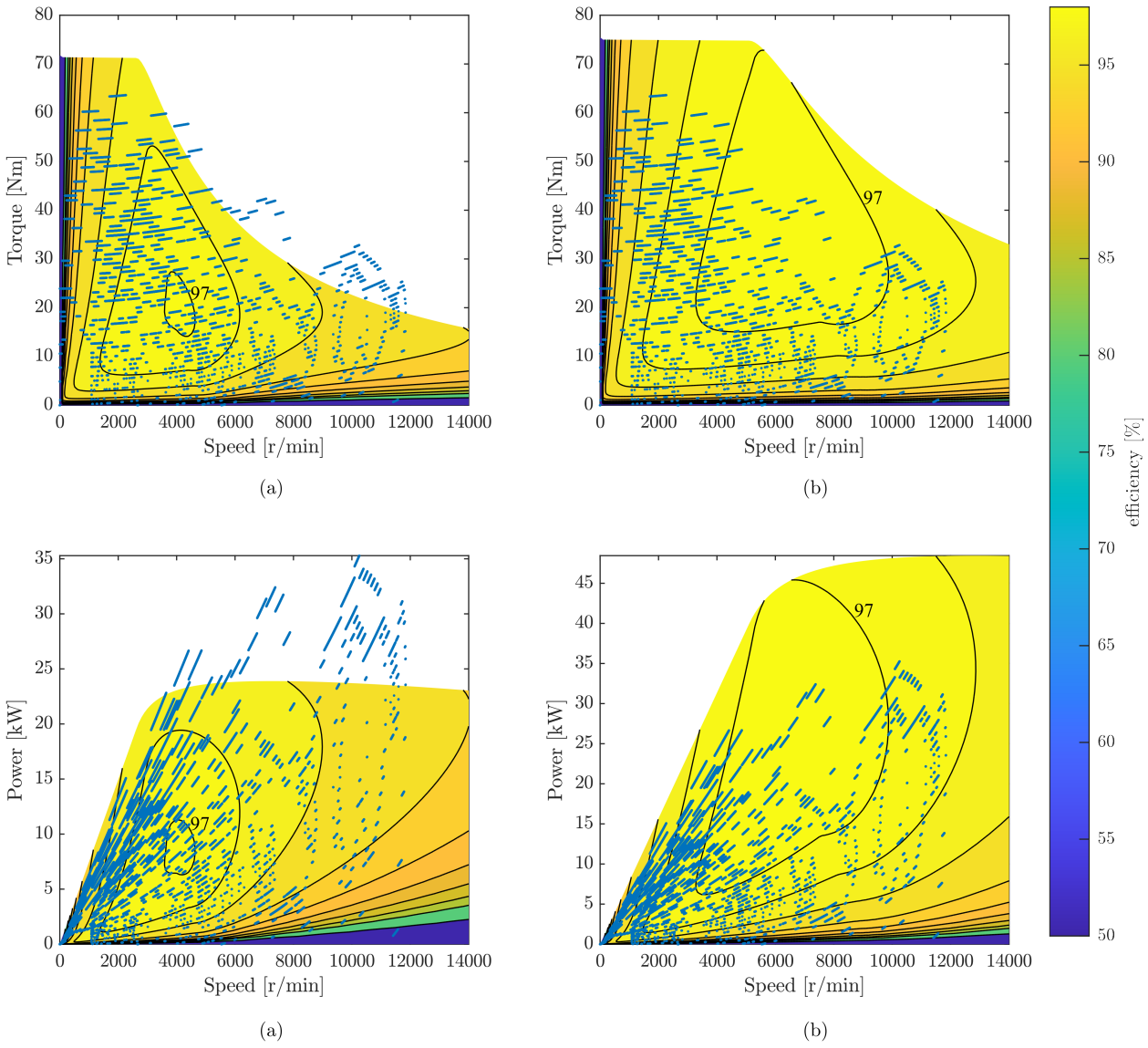


Fig. 7. Torque- and power-speed maps with the WLTP 3 cycle overlapped: (a) three-phase configuration and (b) six-phase configuration. The last contour line corresponding to an efficiency of 97% is displayed.

ting the induced back-EMF of the three-phase in the six-phase connection. Future work points toward geometry optimization based on a driving cycle approach, multiphysics analysis based on thermal and mechanical coupling, implementation of the multiphase control, and experimental validation of the prototype.

ACKNOWLEDGMENTS

This activity has been partially financed by the European Union – Next Generation EU - PNRR M4C2, Investimento 1.4 - Avviso n. 3138 del 16/12/2021 - CN00000023 Sustainable Mobility Center (Centro Nazionale per la Mobilità Sostenibile) - CNMS - CUP E13C22000980001.

Irving S. Aguilar-Zamorate is funded by Consejo Nacional de Humanidades, Ciencias y Tecnologias (CONAHCYT) (scholarship 1105077).

REFERENCES

[1] L. Shao, A. E. H. Karci, D. Tavernini, A. Sorniotti, and M. Cheng, "Design approaches and control strategies for energy-efficient electric machines for electric vehicles—a review," *IEEE Access*, vol. 8, pp. 116 900–116 913, 2020.

[2] A. Bretones, O. Marquet, C. Daher, and L. Hidalgo, "Public health-led insights on electric micro-mobility adoption and use: a scoping review," *Journal of Urban Health*, 2023, accessed: 2024-05-13. [Online]. Available: https://link.springer.com/article/10.1007/s11524-023-00731-0

[3] European Council, "Regulation (EU) No 168/2013 of the European Parliament and of the Council of 15 January 2013 on the approval and market surveillance of two- or three-wheel vehicles and quadricycles," 2013, Official Journal of the European Union. [Online]. Available: https://eur-lex.europa.eu/legal-content/EN/TXT/uri=CELEX:3A32013R0168

[4] R. Manca, E. Tramacere, S. Favelli, A. Tonoli, and L. Camosi, "Impact of rolling resistance modeling on energy consumption for a low voltage battery electric vehicle," in *2023 International Symposium on Electromobility (ISEM)*. IEEE, 2023, pp. 1–6.

[5] European Commission, "Vehicle categories," 2024, https://single-market-economy.ec.europa.eu/sectors/automotive-industry/vehicle-categories_en [Accessed: (26 August 2024)].

[6] A. Salem and M. Narimani, "A Review on Multiphase Drives for Automotive Traction Applications," *IEEE Transactions on Transportation Electrification*, vol. 5, no. 4, pp. 1329–1348, Dec. 2019, conference Name: IEEE Transactions on Transportation Electrification.

[7] A. Negahdari, A. G. Yepes, J. Doval-Gandoy, and H. A. Toliyat, "Efficiency enhancement of multiphase electric drives at light-load operation considering both converter and stator copper losses," *IEEE Transactions on Power Electronics*, vol. 34, no. 2, pp. 1518–1525, 2018.

[8] M. S. Diab, A. A. Elserougi, A. S. Abdel-Khalik, A. M. Massoud, and S. Ahmed, "A Nine-Switch-Converter-Based Integrated Motor Drive and Battery Charger System for EVs Using Symmetrical Six-Phase Machines," *IEEE Transactions on Industrial Electronics*, vol. 63, no. 9, pp. 5326–5335, Sep. 2016, conference Name: IEEE Transactions on Industrial Electronics. [Online]. Available: https://ieeexplore.ieee.org/abstract/document/7454736

[9] Dana TM4, "TM4 Sumo MD," 2024, https://www.danatm4.com/products/systems/sumo-md/ [Accessed: 17 June 2024].

[10] A. Patzak, F. Bachheibl, A. Baumgardt, G. Dajaku, O. Moros, and D. Gerling, "Driving range evaluation of a multi-phase drive for low voltage high power electric vehicles," in *2015 International Conference on Sustainable Mobility Applications, Renewables and Technology (SMART)*, Nov. 2015, pp. 1–7. [Online]. Available: https://ieeexplore.ieee.org/abstract/document/7399237

[11] R. Bojoi, A. Cavagnino, M. Cossale, A. Tenconi, and S. Vaschetto, "Design Trade-off and Experimental Validation of multiphase starter generators for 48V mini-hybrid powertrain," in *2014 IEEE International Electric Vehicle Conference (IEVC)*. Florence: IEEE, Dec. 2014, pp. 1–7. [Online]. Available: https://ieeexplore.ieee.org/document/7056179/

[12] A. Patzak and D. Gerling, "Design of a multi-phase inverter for low voltage high power electric vehicles," in *2014 IEEE International Electric Vehicle Conference (IEVC)*. IEEE, 2014, pp. 1–7.

[13] W. N. W. A. Munim, M. J. Duran, H. S. Che, M. Bermúdez, I. González-Prieto, and N. A. Rahim, "A Unified Analysis of the Fault Tolerance Capability in Six-Phase Induction Motor Drives," *IEEE Transactions on Power Electronics*, vol. 32, no. 10, pp. 7824–7836, Oct. 2017, conference Name: IEEE Transactions on Power Electronics. [Online]. Available: https://ieeexplore.ieee.org/abstract/document/7755726

[14] T. Miller, "Field-weakening performance of brushless synchronous ac motor drives," *IEE Proceedings-Electric Power Applications*, vol. 141, no. 6, pp. 331–340, 1994.

[15] R. Krishnan, *Permanent magnet synchronous and brushless DC motor drives*. Boca Raton: CRC Press/Taylor & Francis, 2010.

[16] Ansys, Inc., "Ansys Motor-CAD." [Online]. Available: https://www.ansys.com/products/electronics/ansys-motor-cad#tab1-1

[17] G. Bertotti, "General properties of power losses in soft ferromagnetic materials," *IEEE Transactions on Magnetics*, vol. 24, no. 1, pp. 621–630, Jan. 1988, conference Name: IEEE Transactions on Magnetics. [Online]. Available: https://ieeexplore.ieee.org/document/43994

[18] D. Ishak, Z. Zhu, and D. Howe, "Eddy-current loss in the rotor magnets of permanent-magnet brushless machines having a fractional number of slots per pole," *IEEE Transactions on Magnetics*, vol. 41, no. 9, pp. 2462–2469, Sep. 2005, conference Name: IEEE Transactions on Magnetics. [Online]. Available: https://ieeexplore.ieee.org/abstract/document/1506916

[19] Z. Liu, Y. Li, and Z. Zheng, "A review of drive techniques for multiphase machines," *CES Transactions on Electrical Machines and Systems*, vol. 2, no. 2, pp. 243–251, Jun. 2018, conference Name: CES Transactions on Electrical Machines and Systems. [Online]. Available: https://ieeexplore.ieee.org/abstract/document/8407074

[20] E. Levi, "Multiphase Electric Machines for Variable-Speed Applications," *IEEE Transactions on Industrial Electronics*, vol. 55, no. 5, pp. 1893–1909, May 2008, conference Name: IEEE Transactions on Industrial Electronics. [Online]. Available: https://ieeexplore.ieee.org/document/4454446